Volume 52
Number 25
7 July 2023
Pages 8491-8820

Dalton Transactions

An international journal of inorganic chemistry

rsc.li/dalton

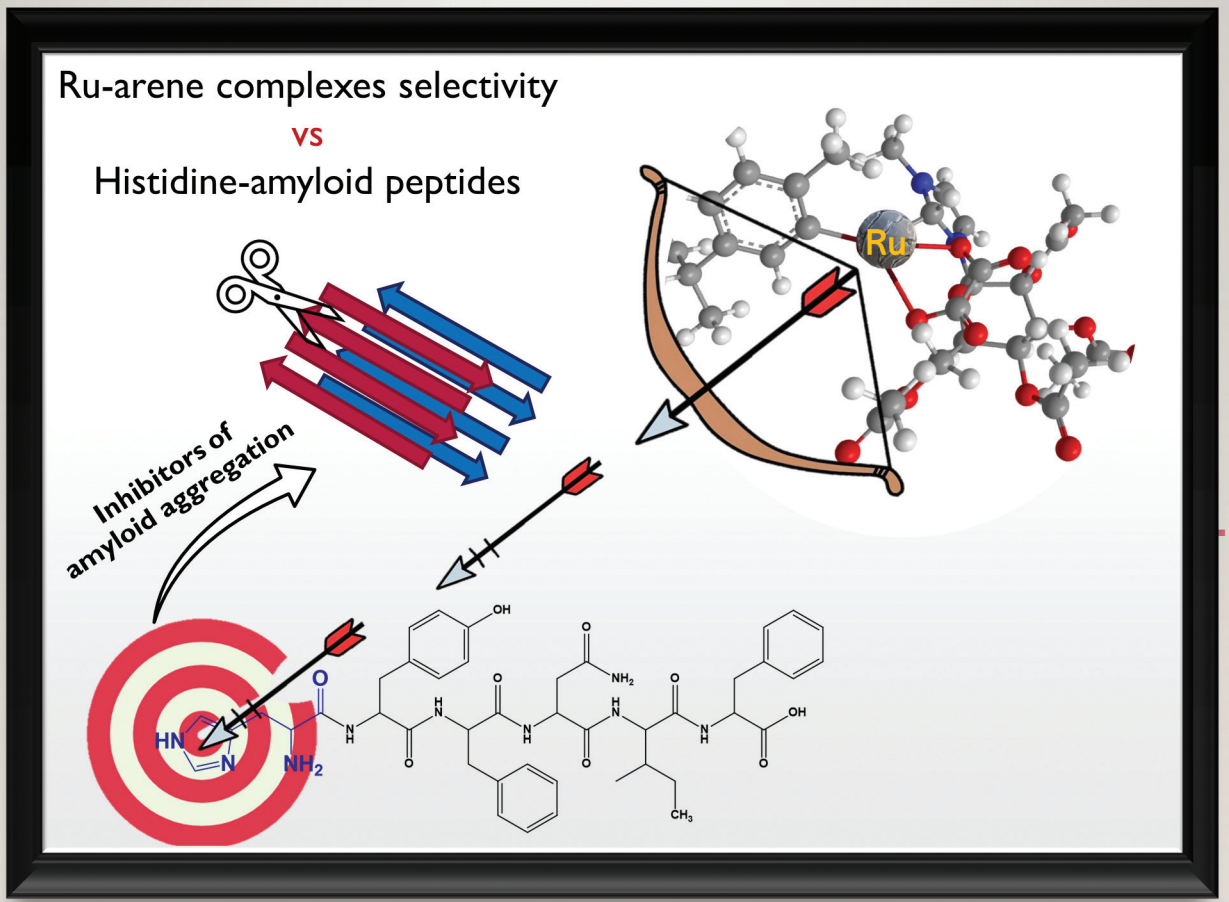

ISSN 1477-9226

ROYAL SOCIETY OF CHEMISTRY

PAPER

Daniela Marasco *et al.*

Ruthenium complexes bearing glucosyl ligands are able to inhibit the amyloid aggregation of short histidine-peptides

Dalton Transactions

ROYAL SOCIETY OF CHEMISTRY

PAPER

View Article Online
View Journal | View Issue

Check for updates

Cite this: *Dalton Trans.*, 2023, **52**, 8549

Ruthenium complexes bearing glucosyl ligands are able to inhibit the amyloid aggregation of short histidine-peptides†

Daniele Florio,[a] Sara La Manna,[a] Alfonso Annunziata,[b] Ilaria Iacobucci,[b,c] Vittoria Monaco,[b,c] Concetta Di Natale,[d] Valentina Mollo,[e] Francesco Ruffo,[b] Maria Monti[b,c] and Daniela Marasco *[a]

Received 12th April 2023,
Accepted 21st May 2023

DOI: 10.1039/d3dt01110k

rsc.li/dalton

Neurodegenerative diseases are often characterized by the formation of aggregates of amyloidogenic peptides and proteins, facilitating the formation of neurofibrillary plaques. In this study, we investigate a series of Ru-complexes sharing three-legged piano-stool structures based on the arene ring and glucosylated carbene ligands. The ability of these complexes to bind amyloid His-peptides was evaluated by ESI-MS, and their effects on the aggregation process were investigated through ThT and Tyr fluorescence emission. The complexes were demonstrated to bind the amyloidogenic peptides even with different mechanisms and kinetics depending on the chemical nature of the ligands around the Ru(II) ion. TEM analysis detected the disaggregation of typical fibers caused by the presence of Ru-compounds. Overall, our results show that the Ru-complexes can modulate the aggregation of His-amyloids and can be conceived as good lead compounds in the field of novel anti-aggregating agents in neurodegeneration.

Introduction

Metallodrugs exhibit interesting pharmacological properties mainly through the substitution processes of ligands and/or redox reactions that characterize their mechanisms of action (MOAs), even if they often result in the multi-targeting and lacking of selectivity.[1] By focusing on the early-stage phases of *in vitro* drug discovery, structure–activity relationship (SAR) investigations can provide crucial insights for the applications of metallodrugs and the identification of their targets.[2]

As is commonly accepted, diverse mechanisms concur in neurodegenerative diseases (NDDs).[3] Thus, a wide range of compounds have been explored as therapeutics.[4] Among the others, transition metal complexes appeared to be good starting compounds for the development of novel neuroprotective-agents.[5,6]

Ruthenium-complexes are in clinical trials for the treatment of several cancers[7] owing to their ability to overcome cisplatin resistance and low general toxicity,[8] and recently they are being applied in NDDs.[9] In a pioneering study, six Ru complexes, containing alternative chloride and aromatic ligands, revealed the capability at different extents to bind the fragment 106–126 of the prion protein, PrP106–126.[10]

In the context of Alzheimer's disease (AD), the PMRU-CYM0 compound (2-aminothiazolium[*trans*-$RuCl_4$(2-aminothiazole)$_2$]) was found to be effective in the modulation of $A\beta_{1-42}$ aggregation with low toxicity.[11]

Other studies outlined that Ru-complexes bearing thiazole ligands were more able to inhibit $A\beta_{1-42}$ aggregation with respect to NAMI-A (imidazolium[*trans*-$RuCl_4$(1*H*-imidazole)(dimethyl sulfoxide-S)]), underlying the importance of secondary interaction spheres between the metallotherapeutic effect and the amyloid peptide,[12,13] similarly to other Ru-complexes bearing the pyridine ligand.[14] Indeed, polypyridyl ligands around the Ru-center [2,2′-bipyridine (bpy), 1,10-phenanthroline (phen), dipyrido[3,2-*a*:2′,3′-*c*]quinolino[3,2-*j*]phenazine (dpqp), quinoxaline (dpq), and dipyridophenazine (dppz)], were found to be efficient in the modulation of the aggregation of human islet amyloid polypeptide (hIAPP) by means of hydrophobic interactions within the metal coordination sphere. In this context, aromatic moieties promoted the disag-

[a]*Department of Pharmacy, University of Naples Federico II, 80131 Naples, Italy. E-mail: daniela.marasco@unina.it; Tel: +39-081-2532043*
[b]*Department of Chemical Sciences, University of Naples Federico II, 80126 Naples, Italy*
[c]*CEINGE Biotecnologie Avanzate "Franco Salvatore" S.c.a r.l., 80131 Naples, Italy*
[d]*Interdisciplinary Research Centre on Biomaterials (CRIB), Department of Ingegneria Chimica del Materiali e della Produzione Industriale (DICMAPI), University Federico II, 80125 Naples, Italy*
[e]*Center for Advanced Biomaterials for Healthcare, Istituto Italiano di Tecnologia (IIT), Largo Barsanti e Matteucci 53, Naples 80125, Italy*

†Electronic supplementary information (ESI) available: Overlay of ThT fluorescence emission intensity of Ru(II)-arene complexes; aromatic intrinsic fluorescence assay of Ru(II)-arene complexes; conformational analysis of Ru(II)-arene complexes; TEM analysis of β_2m_{83-88} peptide alone and in presence of Ru(II)-arene complexes. See DOI: https://doi.org/10.1039/d3dt01110k

gregation of fibrils by changing the β-sheet components and their reduction into small aggregates.[15,16]

Hetero-binuclear Pt–Ru complexes containing bpy and pyrazine (pyz) ligands also were shown to bind hIAPP in an enthalpy-driven process, which was mainly dependent on hydrophobic interactions and changes in the metal coordination.[17]

Very recently, NAMI-A exhibited a dual inhibitory effect toward α-synuclein in both aggregation and membrane interactions, which led to the mitigation of neurodegeneration and motor impairments in a rat model of Parkinson's.[18]

One of the most interesting features of Ru-compounds is their photo-responsiveness:[19] the {$[Ru(bpy)_3]^{2+}$} complex revealed a sensitive, biocompatible, anti-Aβ agent that was able to destabilize the β-sheet conformation upon illumination, causing oxidative modifications of Aβ peptides and aiding the disaggregation effect.[20] Similarly, the luminescent *cis*-$[Ru(phen)_2(Apy)_2]^{2+}$ (Apy = 3,4-diaminopyridine) complex inhibited the aggregation and the toxicity of $A\beta_{1-40}$ and its several fragments.[21] It was also employed as a probe for the detection of fibrillar insulin.[22,23] Similarly, the complex {$[Ru(bpy)_2(dpqp)]^{2+}$} has a luminescence anisotropy that allows for the tracking of the formation of amyloid oligomers at different time points for Aβ and α-synuclein,[24] leading to in-cell mechanistic insights in the early stages of amyloid formation.[25]

Binding analyses through mass spectrometry (MS) revealed for several Ru-complexes a preferential affinity for histidine residues of the N-terminal fragment of the β-amyloid (residues 1–16), in accordance with the binding sites of other metallodrugs such as RAPTA-C and auranofin.[26]

In our previous studies, we investigated the ability of a series of square-planar Pt(II)-complexes to inhibit the aggregation of amyloid peptides, assumed as model amyloids.[27–30] However, a five-coordinate trigonal bipyramidal glucoconjugate Pt(II) complex also was demonstrated to be an efficient inhibitor of β-amyloid fragments.[31] Noticeably, the decoration of organometallic compounds with bioactive moieties able to recognize specific targets is a valid strategy to increase the biological performance of the therapeutic agents. Glycoconjugation is one of the most successful approaches[32–41] because the presence of sugar residues can increase the selectivity through the Warburg effect,[42] the aqueous solubility, and their biocompatibility in general.

Generally, penta- and hexa-peptides as fragments of neurodegenerative proteins were demonstrated to self-assemble, and form amyloids with various morphologies[43,44] that partially recapitulate the aggregation process of larger proteins.[45,46] Herein, we analyzed two different short protein fragments bearing one His residue, assumed as amyloid models, that were both uncharged at neutral pH (Table 1): (i) the fragment 27–32 of the human Bloom syndrome protein (BSP_{27-32}),[47] and (ii) the 103–108 segment of human beta-2-microglobulin that becomes 83–88 (β_2m_{83-88}), after proteolytic cleavage.[43]

Both protein fragments, not present *in vivo*, were identified as aggregation-prone regions (APRs) through prediction and experimental studies.[48,49] The latter sequence does not display "aromatic" amino acids, such as Phe and Tyr,[48] which is different from BSP_{27-32}. These fragments present the ability to aggregate in an amyloid-way, despite their shortness and the presence of His residues as potential ligands to the ruthenium–metal center. Thus, they were assumed as amyloid models in this study, as already reported elsewhere.[50,51]

Table 1 Sequences of His-containing peptides investigated in this study

Peptide	Sequence
BSP_{27-32}	Ac-HYFNIF-NH_2
β_2m_{83-88}	Ac-NHVTLS-NH_2

We evaluated the ability of three Ru-arene complexes[52] containing glucosylated ligands to modulate the aggregative mechanism of amyloid models. The complexes have the general formula $[Ru(\eta^6\text{-arene})(NHC)(X_2)]$ (η^6-arene = *p*-cymene (Cym) or methyl 2-benzamido-3,4,6-tri-*O*-acetyl-beta-D-glucoside (MBAG), NHC = N-heterocyclic carbene, containing a glucosyl and a methyl substituent, $X_2 = Cl^-$ or oxalate) endowed with the typical three-legged piano-stool structure (Fig. 1).[53]

Notably, these complexes recently demonstrated the ability to bind His residues of model proteins.[52]

The presented studies were carried out by employing a wide range of spectroscopic and biophysical techniques: we evaluated the effects of Ru-complexes on fluorescence emission profiles of ThT for both small amyloids. By means of ESI-MS assays, we evaluated the formation of adducts between amyloids and each Ru-complex, and the effects of their presence on the peptides' conformational preferences by CD spectroscopy and on amyloid fibers through TEM analysis.

Experimental section

Peptide synthesis

Reagents for Solid-Phase Peptide Synthesis (SPPS) were purchased from Iris Biotech (Marktredwitz, Germany), and solvents were procured from Romil (Dublin, Ireland). His-amyloid short peptides were synthesized, amidated at the C-terminus and acetylated at the N-terminus. After purification, the pep-

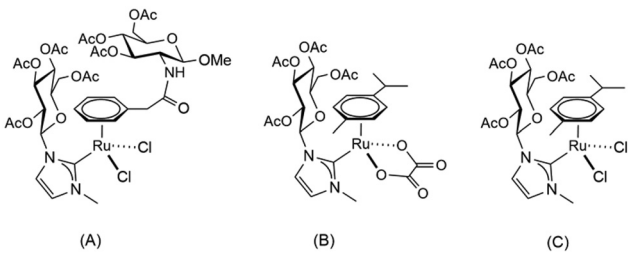

Fig. 1 Chemical structure of the investigated Ru(II)-complexes with NHC *gluco*-conjugated ligands: (A) Ru-MBAG, (B) Ru-Oxa, and (C) Ru-Cym.

tides were treated with 1,1,1,3,3,3-hexafluoro-2-propanol (HFIP) and stored at −20 °C until use.

Ruthenium compounds synthesis and stability

The synthesis and spectroscopic characterization of the Ru(II) complexes have been reported elsewhere.[52]

Briefly, the appropriate ruthenium arene dimer [Ru(η^6-arene)(Cl_2)]$_2$ (0.55 mmol) was reacted with the silver carbene precursor Ag(NHC)Br (1.1 mmol) in 10 mL of dichloromethane for 48 hours, and protected from light. AgBr was filtered off over a pad of Celite, and the volume of the clear filtrate was reduced to 1–2 mL. The addition of diethyl ether resulted in the precipitation of the products as red-orange microcrystalline solids, washed with ether and dried under vacuum. Yields: 75–85%. The stability of the Ru-complexes was assessed by ^{1}H-NMR and ESI-MS, by keeping the complexes over 3 days at 37 °C in aqueous solutions (H_2O or NaCl, 150 mM). Complexes Ru-Cym and Ru-MBAG undergo hydrolysis of one or both chloride ligands, giving rise to an equilibrium involving the mono- and di-aqua species. Ru-Oxa is stable and no appreciable hydrolysis was observed in water nor in NaCl. Ru-MBAG also underwent gradual arene displacement, thus showing reduced stability compared to Ru-Cym and Ru-Oxa. Notably, all the complexes give rise to a slow hydrolysis of the acetyl groups on the sugar fragment in water, while the process occurs faster in basic buffer (Na_2CO_3, pH 12).[52]

Fluorescence assays

Fluorescence assays were performed on a Jasco FP 8300 spectrofluorimeter (Tokyo, Japan) in a 10 mm path-length quartz cuvette under vortex stirring. ThT experiments were performed at 25 °C using a ThT concentration of 50 μM, 10 mM phosphate buffer (pH = 7.4) and a peptide concentration of: 300 μM for $BSP_{27–32}$ and 600 μM for $\beta_2m_{83–88}$ at indicated ratios of Ru-complexes (stock solutions, 50 mM in H_2O). Measurements were collected every 3 min with an excitation wavelength of 440 nm. The emission spectra registered in the 450–600 nm range, and the maximum fluorescence intensity peak was at 483 nm. The aromatic intrinsic fluorescence of $BSP_{27–33}$ (300 μM) alone and at 1 : 5 molar ratio with Ru-complexes was carried out with λ_{exc} = 275 nm and λ_{emi} = 303 nm.

Circular dichroism

The CD spectra of $\beta_2m_{83–88}$ (400 μM, in 10 mM phosphate buffer) alone and with Ru-complexes at a 1 : 1 peptide-to-metal complex molar ratio, were registered at indicated times on a J-810 spectropolarimeter (JASCO Corp., Milan, Italy), in a 0.1 cm cuvette at 25 °C in the far-UV region from 190 to 260 nm. Other experimental settings were 20 nm min^{-1} scan speed, 2.0 nm bandwidth, 0.2 nm resolution, 50 mdeg sensitivity, and 4 s response.

ESI-MS analysis

Solutions of $BSP_{27–32}$ and $\beta_2m_{83–88}$ peptides with a concentration of 50 μM in 15 mM AMAC (ammonium acetate) buffer pH = 7.0, alone and at 1 : 5 peptide : complex molar ratio were incubated at two different times (0 and 24 h), and then analyzed by Q-ToF Premier (Waters, Milliford, MA, USA) mass spectrometer. The isolated peptides and the three Ru-complexes alone were evaluated as the control. The analyses were done by direct injection at 10 μL min^{-1} setting, with the source parameters at 3 kV for capillary voltage and 42 kV for cone voltage. The acquisition range used was from 100 to 2000 m/z, and the raw data were processed with MassLynx 4.1 software (Waters, Milliford, MA, USA).

Transmission electron microscopy

TEM analysis by negative staining was carried out to visualize the morphology of the fibrils and prefibrillar aggregates.[54]

Uranyl acetate and 200 mesh copper grids were purchased from Electron Microscopy Sciences (Hatfield, PA, USA).

Peptides were dissolved at 6.0 and 7.0 mM for $BSP_{27–32}$ and $\beta_2m_{83–88}$, respectively, in 10 mM phosphate and with a peptide/metal complex molar ratio of 1 : 5. At each time point, they were diluted at ∼1 mM. A drop of 10 μL of each sample was placed onto a formvar/carbon copper grid for 2 minutes, and washed two times in drops of distilled water. Negative staining was carried out in a drop of 100 μL of 2% (w/w) uranyl acetate aqueous solution for 2 minutes in the dark. After the incubation time, the excess of liquid was removed by touching the edge to a filter paper, and the grids were air-dried under hood. The imaging was performed by using a TEM Tecnai G2, 20_Thermofisher Company apparatus equipped with a CCD camera (Eagle-2HS), at 120 kV in a range of magnification between 8k× and 150k× (integration time: 1 s; image size 2048 × 2048).

Results and discussion

Effects of ruthenium complexes on $\beta_2m_{83–88}$ and $BSP_{27–32}$ amyloid aggregation

Spectroscopic investigations provided evidence of the ability of metal-complexes to modulate the aggregation of His-amyloid peptides. Thioflavin T (ThT) was used as preferential dye because of its ability to bind to amyloid aggregates.[55]

The overlays of the ThT-fluorescence emission profiles of the His-amyloids in the presence or lack of Ru-compounds over time are reported in Fig. 2A and B.

ThT assays were performed at two different molar ratios of peptide to metal complex, 1 : 1 and 1 : 5. By comparing peptides alone, $BSP_{27–32}$ exhibited the typical amyloid profile with an increase of ThT emission in the first 15 min of analysis and then a slow decrease upon fibrillation.[56]

Conversely, the $\beta_2m_{83–88}$ peptide appeared already aggregated at t = 0 of analysis with a decrease of signal after 5 min.[57]

For both sequences, a decrease of the ThT signal is observed in the presence of Ru-compounds: the most potent inhibitor of aggregation appeared for Ru-Cym. Already at a 1 : 1 ratio, it caused a neat suppression of fluorescence intensity. Meanwhile, both Ru-MBAG and Ru-Oxa at this ratio exhibited

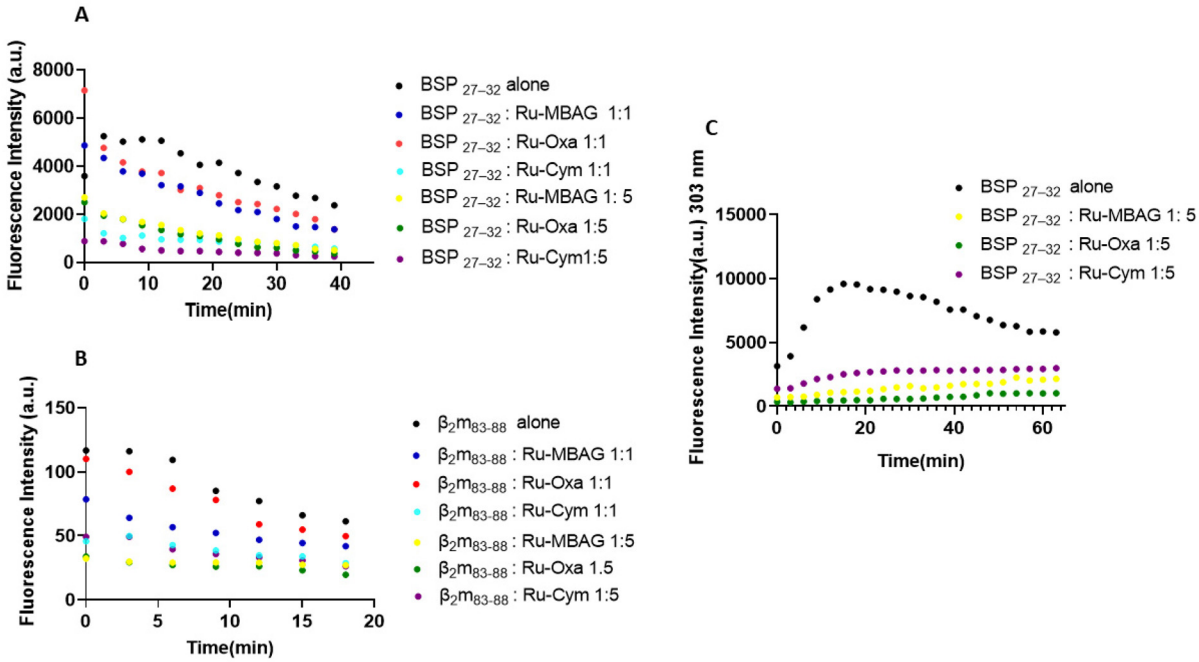

Fig. 2 Time course-fluorescence assays. ThT fluorescence emission intensity of (A) BSP_{27-32} alone (black), (B) β_2m_{83-88} alone (black), and in the presence of Ru-complexes: Ru-Cym at 1 : 1 (light blue) and 1 : 5 (violet), Ru-MBAG at 1 : 1 (blue) and 1 : 5 (yellow), and Ru-Oxa at 1 : 1 (red) and 1 : 5 (green) peptide : complex molar ratios. (C) Aromatic fluorescence emission of BSP_{27-32} alone and in the presence of Ru-complexes at a 1 : 5 molar ratio.

only a small reduction of signal, and required a higher ratio (1 : 5) to provide effects comparable to those of Ru-Cym. Control experiments, reported in Fig. S1,† allowed for the exclusion of any interference due to the interaction of Ru-complexes with ThT. In the case of BSP_{27-32}, the presence of three aromatic residues, F29, F32 and Y28, acts as an additional probe for amyloid aggregation, following the intrinsic fluorescence at 303 nm (upon 275 nm-excitation) during time, as reported in Fig. 2C. BSP_{27-32} alone exhibits an increase of fluorescence intensity, as already observed for aromatic sequences, suggesting a prominent role in π-stacking during fibrillation.[58]

Conversely, the presence of Ru-compounds caused a decrease of fluorescence signal at the beginning of the analysis, corroborating the inhibitory effect on the aggregation. Control experiments, reported in Fig. S2,† indicate a negligible contribution of the emission of Ru compounds upon aromatic excitation.

ESI-MS analysis of the adducts of BSP_{27-32} and β_2m_{83-88} with Ru-complexes

The formation of adducts between Ru-complexes and amyloid peptides was studied by electrospray ionization mass spectrometry (ESI-MS). The three Ru-compounds were incubated at two different times (0 and 24 h) with the two peptides and analyzed. The ESI-MS spectra are reported in: Fig. 3 for Ru-MBAG, Fig. 4 for Ru-Cym and Fig. 5 for Ru-Oxa. As reference, in Fig. S3,† the ESI-MS spectra of peptides alone are reported. In each figure, label A refers to BSP_{27-32} and B to β_2m_{83-88}, while

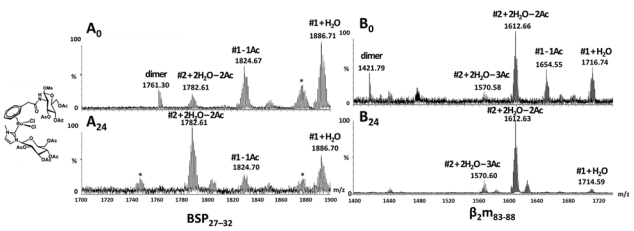

Fig. 3 ESI-MS spectra of mixtures of BSP_{27-32} (A_0, A_{24} panels) and β_2m_{83-88} (B_0, B_{24} panels) with Ru-MBAG. Asterisks label peaks present in the spectra of Ru-MBAG alone.

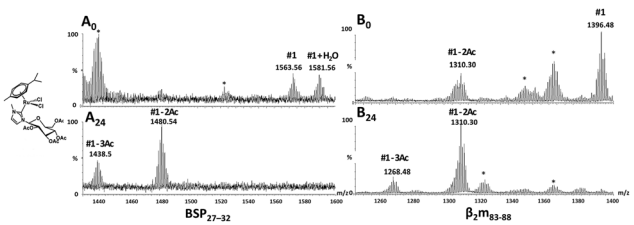

Fig. 4 ESI-MS spectra of mixtures of BSP_{27-32} (A_0, A_{24} panels) and β_2m_{83-88} (B_0, B_{24} panels) with Ru-Cym. Asterisks label peaks present in the spectra of Ru-Cym alone.

subscripts 0 and 24 indicate the times of incubation. All spectra confirmed the formation of adducts with a 1 : 1 stoichiometry. The experimental and theoretical values of ions are reported in Table 2. In the presence of Ru-MBAG and Ru-Cym

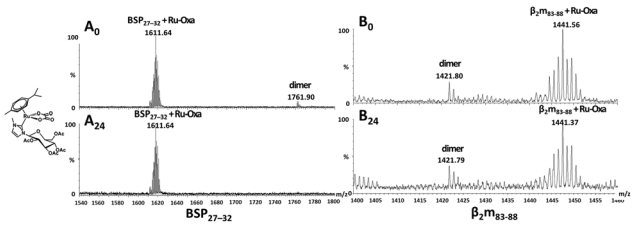

Fig. 5 ESI-MS spectra of mixtures of BSP_{27-32} (A_0, A_{24} panels) and β_2m_{83-88} (B_0, B_{24} panels) with Ru-Oxa. Asterisks label peaks present in the spectra of Ru-Oxa alone.

(Fig. 3 and 4), the spectra presented peaks due to adducts between the peptide and the complexes missing one (peak #1) or two (peak #2) chlorides, already at t = 0 h. Other adducts contained water molecules in the substitution of chloride ions, mainly for Ru-MBAG-adducts. For both Ru-compounds, the simultaneous hydrolysis of acetyl groups of the sugar ligands was evident, as already reported.[52] Only for Ru-MBAG at t = 0, several peaks are due to the presence of dimeric forms of intact peptides. Conversely, the complex Ru-Oxa exhibited peaks due to the formation of adducts with both peptides without losing the oxalate ligand or acetyl groups of glucosyl ligands (Fig. 5). At t = 0, the dimeric species of free peptides were present that persisted at t = 24 h in the case of β_2m_{83-88}.

Conformational effects of ruthenium compounds on His-amyloid peptides

Potential conformational effects induced by Ru-complexes on short sequences were investigated through CD spectroscopy. The β_2m_{83-88} peptide was analyzed in an interval time of ~16 h, alone, and in the presence of the Ru-complexes.

Table 2 Table of single charged monoisotopic ions relative to the adducts of BSP_{27-32} and β_2m_{83-88} with Ru-compounds. 1 and 2 correspond to the adducts peptide/metal complex lacking one and two chlorines, respectively. Times of incubation, experimental and theoretical masses are also reported

	Time	Experimental m/z (z = +1) (Da)	Theoretical monoisotopic mass (Da)	Adducts	
BSP_{27-32} + Ru-MBAG	0 h	881.45	880.41	BSP_{27-32}	
(MW: 1021.8 Da)		1761.90	1760.82	BSP_{27-32} dimer	
		1782.65	1783.22	BSP_{27-32} + Ru-MBAG − $2Cl^-$ + $2H_2O$ − 2Ac	2 + $2H_2O$ − 2Ac
		1824.67	1824.71	BSP_{27-32} + Ru-MBAG − $1Cl^-$ − 1Ac	1 − 1Ac
		1886.71	1884.76	BSP_{27-32} + Ru-MBAG − $1Cl^-$ + $1H_2O$	1 + H_2O
	24 h	881.45	880.41	BSP_{27-32}	
		1782.61	1783.22	BSP_{27-32} + Ru-MBAG − $2Cl^-$ + $2H_2O$ − 2Ac	2 + $2H_2O$ − 2Ac
		1824.70	1824.71	BSP_{27-32} + Ru-MBAG − $1Cl^-$ − 1Ac	1 − 1Ac
		1886.70	1884.76	BSP_{27-32} + Ru-MBAG − $1Cl^-$ + $1H_2O$	1 + H_2O
β_2m_{83-88} + Ru-MBAG	0 h	711.41	710.35	β_2m_{83-88}	
(MW: 1021.8 Da)		1421.79	1420.70	β_2m_{83-88} dimer	
		1570.58	1571.11	β_2m_{83-88} + Ru-MBAG − $2Cl^-$ + $2H_2O$ − 3Ac	2 + $2H_2O$ − 3Ac
		1612.66	1613.16	β_2m_{83-88} + Ru-MBAG − $2Cl^-$ + $2H_2O$ − 2Ac	2 + $2H_2O$ − 2Ac
		1654.55	1654.65	β_2m_{83-88} + Ru-MBAG − $1Cl^-$ − 1Ac	1 − 1Ac
		1716.74	1714.70	β_2m_{83-88} + Ru-MBAG − $1Cl^-$ + $1H_2O$	1 + H_2O
	24 h	711.40	710.35	β_2m_{83-88}	
		1570.60	1571.11	β_2m_{83-88} + Ru-MBAG − $2Cl^-$ + $2H_2O$ − 3Ac	2 + $2H_2O$ − 3Ac
		1612.63	1613.16	β_2m_{83-88} + Ru-MBAG − $2Cl^-$ + $2H_2O$ − 2Ac	2 + $2H_2O$ − 2Ac
		1714.59	1714.70	β_2m_{83-88} + Ru-MBAG − $1Cl^-$ + $1H_2O$	1 + H_2O
BSP_{27-32} + Ru-Cym	0 h	881.42	880.41	BSP_{27-32}	
(MW: 718.6 Da)		1563.56	1563.56	BSP_{27-32} + Ru-Cym − Cl^-	1
		1581.56	1581.56	BSP_{27-32} + Ru-Cym − Cl^- + H_2O	1 + H_2O
	24 h	881.42	880.41	BSP_{27-32}	
		1480.54	1479.56	BSP_{27-32} + Ru-Cym − Cl^- − 2Ac	1 − 2Ac
		1438.5	1437.56	BSP_{27-32} + Ru-Cym − Cl^- − 3Ac	1 − 3Ac
β_2m_{83-88} + Ru-Cym	0 h	711.37	710.35	β_2m_{83-88}	
(MW: 718.6 Da)		1396.48	1393.50	β_2m_{83-88} + Ru-Cym − Cl^-	1
		1310.30	1309.50	β_2m_{83-88} + Ru-Cym − Cl^- − 2Ac	1 − 2Ac
	24 h	711.37	710.35	β_2m_{83-88}	
		1310.3	1309.50	β_2m_{83-88} + Ru-Cym − Cl^- − 2Ac	1 − 2Ac
		1268.48	1267.50	β_2m_{83-88} + Ru-Cym − Cl^- − 3Ac	1 − 3Ac
BSP_{27-32} + Ru-Oxa	0 h	881.46	880.41	BSP_{27-32}	
(MW: 735.7 Da)		1761.90	1760.82	BSP_{27-32} dimer	
		1611.64	1611.57	BSP_{27-32} + Ru-Oxa	
	24 h	881.45	880.41	BSP_{27-32}	
		1611.64	1611.57	BSP_{27-32} + Ru-Oxa	
β_2m_{83-88} + Ru-Oxa	0 h	711.40	710.35	β_2m_{83-88}	
(MW: 735.7 Da)		1421.80	1420.70	β_2m_{83-88} dimer	
		1441.56	1441.51	β_2m_{83-88} + Ru-Oxa	
	24 h	711.39	710.35	β_2m_{83-88}	
		1421.79	1420.70	β_2m_{83-88} dimer	
		1441.37	1441.51	β_2m_{83-88} + Ru-Oxa	

Unfortunately, a similar time course analysis was impossible for BSP_{27-32} because of the high concentration required for CD analysis (1 mM),[59] which caused a fast precipitation of the peptide, providing no significant CD signal (Fig. S4†). As expected, the CD spectrum of β_2m_{83-88} alone at t = 0 did not indicate a well-defined secondary structure, but rather a random state. Over time, the decrease of the CD signal indicated the occurrence of aggregation (Fig. 6A).

The presence of Ru-compounds did not drastically change the spectral profile over time (Fig. 6B–D). However, the presence of complexes allowed for a certain stability of the CD intensity as evaluated from Fig. S5,† in which the CD signals (at the minimum of each spectrum) at different times are reported. In particular, Ru-Cym, at higher times, stabilized the CD signal (and thus the monomeric state) more strongly with respect to other Ru-complexes. The CD profiles of the complexes alone (Fig. S6†) ensure no interference of the complexes on the peptide profile.

Effects of ruthenium compounds on the aggregates' morphology of His amyloids

To gain insights into the morphological effects of the Ru-complexes on the aggregates of amyloid fibers, TEM microscopy was used. The analyses were carried out at two different time points: 0 and 4 days. At t = 0, BSP_{27-32} alone self-assembled into typical amyloid nanofibers (Fig. 7A), and was well defined in length and diameter ($l_{average}$ = ~600 nm, $d_{average}$ = 6.7 ± 1.5 nm). These nanofibers appeared to be completely dissolved in the presence of Ru-Cym and Ru-MBAG complexes (Fig. 7B and C), and partially in the case of the Ru-Oxa complex, where a few fibers were still observable (Fig. 7D). Conversely, after 4 days, the peptide BSP_{27-32} alone exhibited polydisperse amorphous aggregates, as in the presence of Ru-complexes (Fig. S7†). Under similar conditions, the β_2m_{83-88} peptide did not provide fibers but only amorphous oligomers. This is likely due to the co-occurrence of precipitation at the millimolar concentrations used for the preparation of samples (Fig. S8†).

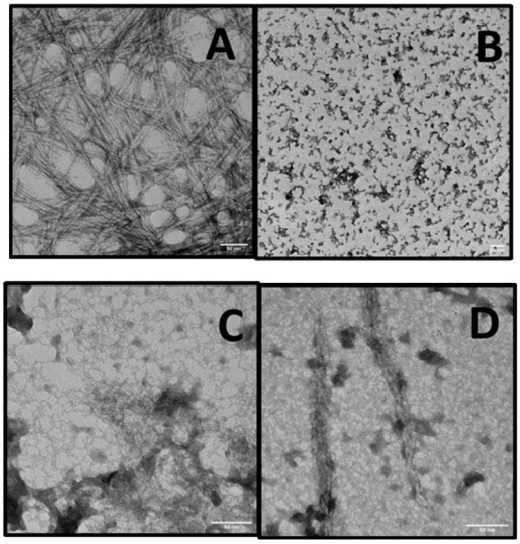

Fig. 7 TEM analysis at t = 0 of the BSP_{27-32} peptide (A) alone, and in the presence of (B) Ru-Cym, (C) Ru-MBAG, and (D) Ru-Oxa.

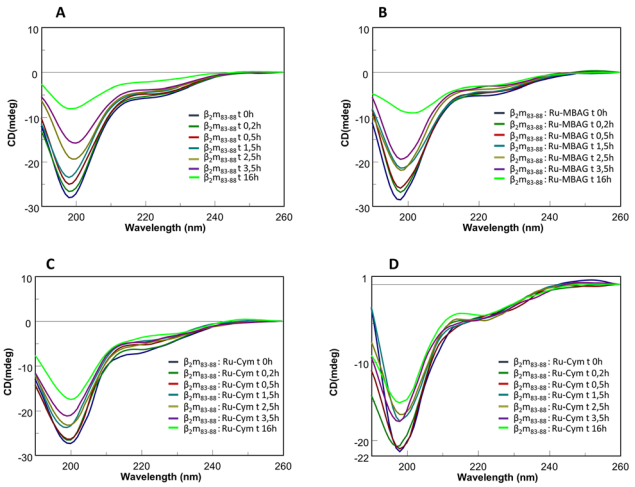

Fig. 6 Conformational analysis of β_2m_{83-88}. Overlay of CD spectra of β_2m_{83-88} (400μM) alone (A) and with Ru-MBAG (B), Ru-Oxa (C) Ru-Cym (D), at 1 : 1 molar ratio.

Conclusions

The present study involves a recent *ad hoc* "drug repurposing" approach: it is a strategy for the identification of new uses for approved or investigational drugs, outside the original medicinal field of application.[60] Ru-based anticancer drugs represent an important class of antineoplastic agents that are often used in orthogonality with Pt-compounds.[61] Recently, in-depth investigations of their MOAs prompted researchers to analyze their efficacy as potential neurodrugs.[27–30,62] Commonly, Ru-complexes, in their interaction with biomolecules, exhibit a preferential propensity to bind the indole side-chain of His residues upon a ligands' exchange mechanism.[26] Herein, we investigated three Ru-complexes, sharing NHC *gluco*-conjugated ligands and differing in the nature of η^6-arene ligands (*p*-cymene or methyl 2-benzamido-3,4,6-tri-*O*-acetyl-beta-D-glucoside), or in the presence of chlorides or bidentate oxalate as the anionic ligands. Ru-MBAG contained an additional glucosyl moiety on the arene ring (Fig. 1). The abilities of these Ru-compounds to modulate amyloid aggregation were tested on two short His-peptides with and without aromatic residues, which are small fragments (BSP_{27-32} and β_2m_{83-88}) of neurodegenerative proteins that demonstrated nucleation sites of amyloid aggregation of larger polypeptides.[63] All three complexes in the ThT assays affected the fluorescence time courses: a clear suppression of the aggregation was observable with a greater effect exhibited by Ru-Cym, which acted as an inhibitor already at 1 : 1 peptide : complex molar ratio, with no substantial variation at 1 : 5 ratio. In comparison, other com-

plexes demonstrated dose-dependent inhibitory effects. In the ESI-MS experiments outlined for the chloride complexes, *i.e.*, Ru-Cym and Ru-MBAG, there was a formation of adducts involving the loss of chloride ions, in addition to the hydrolysis of acetyl groups of glucosyl ligands.

Conversely, the ESI data of Ru-Oxa indicated no ligand exchange. This behavior is likely due to the chelate stabilizing effect of oxalate with respect to monodentate chlorides that hampers the ligands' exchange around the Ru center,[64] as already observed during stability assays, allowing only electrostatic and/or hydrophobic interactions for the formation of adducts with peptides.

The choice of short His-amyloid peptides as model amyloids markedly simplified the synthesis and purification of the amyloidogenic systems, but simultaneously severely limited the conformational studies. Indeed, CD analysis allowed us to only assess a substantial stabilization of the monomeric form of the β_2m_{83-88} peptide, especially in the presence of Ru-Cym. However, the conformational mechanisms cannot be detailed in-depth for such small peptides. Future investigations on larger polypeptides containing His-residues are required to translate into the observed inhibitory effects produced by the Ru-complexes on biological processes, and also to evaluate the inhibition of the amyloid cytotoxicity, considering that Ru-complexes were not toxic up to 100 μM in many cell lines.[52]

Finally, microscopy TEM investigations confirmed an immediate effect of Ru-Cym and Ru-MBAG on the amyloidogenicity of the BSP_{27-32} peptide, causing a neat dispersing effect on the typical fibers observable in their absence.

In conclusion, this study represents an interesting example of how *in vitro* SAR investigations of the MOAs of metallodrugs on amyloid systems can be of utmost importance for the employment of analogous glycoconjugate Ru-complexes as novel and selective drugs in neurodegenerative diseases.

Author contributions

D. F. and S. L. M. synthesized the peptides and performed the fluorescence and CD studies, I. I., V. M. and M. M. performed the ESI-experiments, C. D. N. and V. M. did the TEM assays, A. A. and F. R. synthesized and characterized the metal complexes, D. M. and F. R. designed the concept and supervised the experiments. D. M. wrote the manuscript. All authors have read and approved the final version of the manuscript.

Conflicts of interest

The authors declare no competing interests.

Acknowledgements

This work was supported by Associazione Italiana per la Ricerca sul Cancro (AIRC) grant IG 2022, Rif. 27378 (D. M.) and by #NEXTGENERATIONEU (NGEU), Ministry of University and Research (MUR), National Recovery and Resilience Plan (NRRP), project MNESYS (PE0000006) – A Multiscale integrated approach to the study of the nervous system in health and disease (DN. 1553 11.10.2022).

References

1 E. Fotopoulou, I. Titilas and L. Ronconi, *Recent Pat. Anti-Cancer Drug Discovery*, 2022, **17**, 42–54.
2 E. J. Anthony, E. M. Bolitho, H. E. Bridgewater, O. W. Carter, J. M. Donnelly, C. Imberti, E. C. Lant, F. Lermyte, R. J. Needham and M. Palau, *Chem. Sci.*, 2020, **11**, 12888–12917.
3 J. A. Santiago, V. Bottero and J. A. Potashkin, *Front. Aging Neurosci.*, 2017, **9**, 166.
4 P. C. Trippier, K. Jansen Labby, D. D. Hawker, J. J. Mataka and R. B. Silverman, *J. Med. Chem.*, 2013, **56**, 3121–3147.
5 K. D. Mjos and C. Orvig, *Chem. Rev.*, 2014, **114**, 4540–4563.
6 J. S. Derrick, J. Lee, S. J. C. Lee, Y. Kim, E. Nam, H. Tak, J. Kang, M. Lee, S. H. Kim and K. Park, *J. Am. Chem. Soc.*, 2017, **139**, 2234–2244.
7 E. Alessio and L. Messori, *Metallo-Drugs: Development and Action of Anticancer Agents*, 2018, vol. 18. ISBN: 9783110470734.
8 T. A. Sales, I. G. Prandi, A. A. de Castro, D. H. Leal, E. F. da Cunha, K. Kuca and T. C. Ramalho, *Int. J. Mol. Sci.*, 2019, **20**, 1829.
9 F. V. G. Justi, G. A. Matos, J. d. S. R. Caminha, C. R. Roque, E. M. Carvalho, M. W. S. Campelo, L. Belayev, L. G. de França Lopes and R. B. Oriá, *J. Pharmacol. Exp. Ther.*, 2022, **380**, 47–53.
10 X. Wang, B. Zhang, C. Zhao, Y. Wang, L. He, M. Cui, X. Zhu and W. Du, *J. Inorg. Biochem.*, 2013, **128**, 1–10.
11 L. Messori, M. Camarri, T. Ferraro, C. Gabbiani and D. Franceschini, *ACS Med. Chem. Lett.*, 2013, **4**, 329–332.
12 G. K. Yawson, S. E. Huffman, S. S. Fisher, P. J. Bothwell, D. C. Platt, M. A. Jones, G. M. Ferrence, C. G. Hamaker and M. I. Webb, *J. Inorg. Biochem.*, 2021, **214**, 111303.
13 S. E. Huffman, G. K. Yawson, S. S. Fisher, P. J. Bothwell, D. C. Platt, M. A. Jones, C. G. Hamaker and M. I. Webb, *Metallomics*, 2020, **12**, 491–503.
14 B. J. Wall, M. F. Will, G. K. Yawson, P. J. Bothwell, D. C. Platt, C. F. Apuzzo, M. A. Jones, G. M. Ferrence and M. I. Webb, *J. Med. Chem.*, 2021, **64**, 10124–10138.
15 D. Zhu, G. Gong, W. Wang and W. Du, *J. Inorg. Biochem.*, 2017, **170**, 109–116.
16 G. Gong, J. Xu, X. Huang and W. Du, *JBIC, J. Biol. Inorg. Chem.*, 2019, **24**, 179–189.
17 G. Gong, W. Du, J. Xu, X. Huang and G. Yin, *J. Inorg. Biochem.*, 2018, **189**, 7–16.
18 K. Cao, Y. Zhu, Z. Hou, M. Liu, Y. Yang, H. Hu, Y. Dai, Y. Wang, S. Yuan and G. Huang, *Angew. Chem., Int. Ed.*, 2023, **62**, e202215360.
19 L. Conti, E. Macedi, C. Giorgi, B. Valtancoli and V. Fusi, *Coord. Chem. Rev.*, 2022, **469**, 214656.

20 G. Son, B. I. Lee, Y. J. Chung and C. B. Park, *Acta Biomater.*, 2018, **67**, 147–155.
21 M. P. Cali, L. M. Pereira, M. D. Teodoro, T. A. Sellani, E. G. Rodrigues and R. M. Carlos, *J. Inorg. Biochem.*, 2021, **215**, 111314.
22 L. M. Pereira, M. P. Cali, R. C. Marchi, W. M. Pazin and R. M. Carlos, *J. Inorg. Biochem.*, 2021, **224**, 111585.
23 D. E. Silva, M. P. Cali, W. M. Pazin, E. Carlos-Lima, M. T. Salles Trevisan, T. Venancio, M. Arcisio-Miranda, A. S. Ito and R. M. Carlos, *J. Med. Chem.*, 2016, **59**, 9215–9227.
24 B. Jiang, A. Aliyan, N. P. Cook, A. Augustine, G. Bhak, R. Maldonado, A. D. Smith McWilliams, E. M. Flores, N. Mendez and M. Shahnawaz, *J. Am. Chem. Soc.*, 2019, **141**, 15605–15610.
25 J.-Y. Shao, S.-H. Wu, J. Ma, Z.-L. Gong, T.-G. Sun, Y. Jin, R. Yang, B. Sun and Y.-W. Zhong, *Chem. Commun.*, 2020, **56**, 2087–2090.
26 L. K. Batchelor, D. Ortiz and P. J. Dyson, *Inorg. Chem.*, 2019, **58**, 2501–2513.
27 D. Florio, I. Iacobucci, G. Ferraro, A. M. Mansour, G. Morelli, M. Monti, A. Merlino and D. Marasco, *Pharmaceuticals*, 2019, **12**, 154.
28 D. Florio, A. M. Malfitano, S. Di Somma, C. Mügge, W. Weigand, G. Ferraro, I. Iacobucci, M. Monti, G. Morelli and A. Merlino, *Int. J. Mol. Sci.*, 2019, **20**, 829.
29 D. Florio, M. Cuomo, I. Iacobucci, G. Ferraro, A. M. Mansour, M. Monti, A. Merlino and D. Marasco, *Pharmaceuticals*, 2020, **13**, 171.
30 S. L. Manna, D. Florio, I. Iacobucci, F. Napolitano, I. D. Benedictis, A. M. Malfitano, M. Monti, M. Ravera, E. Gabano and D. Marasco, *Int. J. Mol. Sci.*, 2021, **22**, 3015.
31 S. La Manna, M. Leone, I. Iacobucci, A. Annuziata, C. Di Natale, E. Lagreca, A. M. Malfitano, F. Ruffo, A. Merlino and M. Monti, *Inorg. Chem.*, 2022, **61**, 3540–3552.
32 Y. Chen, M. J. Heeg, P. G. Braunschweiger, W. Xie and P. G. Wang, *Angew. Chem., Int. Ed.*, 1999, **38**, 1768–1769.
33 M. Gottschaldt and U. S. Schubert, *Chem. – Eur. J.*, 2009, **15**, 1548–1557.
34 P. Liu, Y. Lu, X. Gao, R. Liu, D. Zhang-Negrerie, Y. Shi, Y. Wang, S. Wang and Q. Gao, *Chem. Commun.*, 2013, **49**, 2421–2423.
35 M. Vaccaro, R. Del Litto, G. Mangiapia, A. M. Carnerup, G. D'Errico, F. Ruffo and L. Paduano, *Chem. Commun.*, 2009, 1404–1406.
36 M. E. Cucciolito, A. D'Amora, G. De Feo, G. Ferraro, A. Giorgio, G. Petruk, D. M. Monti, A. Merlino and F. Ruffo, *Inorg. Chem.*, 2018, **57**, 3133–3143.
37 M. E. Cucciolito, F. D. L. Bossa, R. Esposito, G. Ferraro, A. Iadonisi, G. Petruk, L. D'Elia, C. Romanetti, S. Traboni and A. Tuzi, *Inorg. Chem. Front.*, 2018, **5**, 2921–2933.
38 A. Annunziata, M. E. Cucciolito, R. Esposito, P. Imbimbo, G. Petruk, G. Ferraro, V. Pinto, A. Tuzi, D. M. Monti and A. Merlino, *Dalton Trans.*, 2019, **48**, 7794–7800.
39 A. Annunziata, A. Amoresano, M. E. Cucciolito, R. Esposito, G. Ferraro, I. Iacobucci, P. Imbimbo, R. Lucignano, M. Melchiorre and M. Monti, *Inorg. Chem.*, 2020, **59**, 4002–4014.
40 A. Annunziata, M. E. Cucciolito, R. Esposito, G. Ferraro, D. M. Monti, A. Merlino and F. Ruffo, *Eur. J. Inorg. Chem.*, 2020, 918–929.
41 A. Annunziata, M. E. Cucciolito, P. Imbimbo, A. Silipo and F. Ruffo, *Inorg. Chim. Acta*, 2021, **516**, 120092.
42 M. Patra, T. C. Johnstone, K. Suntharalingam and S. J. Lippard, *Angew. Chem.*, 2016, **128**, 2596–2600.
43 Z. S. Al-Garawi, K. L. Morris, K. E. Marshall, J. Eichler and L. C. Serpell, *Interface Focus*, 2017, **7**, 20170027.
44 P. L. Scognamiglio, C. Di Natale, G. Perretta and D. Marasco, *Curr. Med. Chem.*, 2013, **20**, 3803–3817.
45 L. M. Hawk, J. M. Pittman, P. C. Moore, A. K. Srivastava, J. Zerweck, J. T. Williams, A. J. Hawk, J. R. Sachleben and S. C. Meredith, *Protein Sci.*, 2020, **29**, 527–541.
46 M. L. Giuffrida, G. Grasso, M. Ruvo, C. Pedone, A. Saporito, D. Marasco, B. Pignataro, C. Cascio, A. Copani and E. Rizzarelli, *J. Neurosci. Res.*, 2007, **85**, 623–633.
47 K. L. Morris, A. Rodger, M. R. Hicks, M. Debulpaep, J. Schymkowitz, F. Rousseau and L. C. Serpell, *Biochem. J.*, 2013, **450**, 275–283.
48 M. I. Ivanova, M. R. Sawaya, M. Gingery, A. Attinger and D. Eisenberg, *Proc. Natl. Acad. Sci. U. S. A.*, 2004, **101**, 10584–10589.
49 S. Maurer-Stroh, M. Debulpaep, N. Kuemmerer, M. L. De La Paz, I. C. Martins, J. Reumers, K. L. Morris, A. Copland, L. Serpell and L. Serrano, *Nat. Methods*, 2010, **7**, 237–242.
50 L. D. Aubrey, B. J. Blakeman, L. Lutter, C. J. Serpell, M. F. Tuite, L. C. Serpell and W.-F. Xue, *Commun. Chem.*, 2020, **3**, 125.
51 S.-R. Meng, Y.-Z. Zhu, T. Guo, X.-L. Liu, J. Chen and Y. Liang, *PLoS One*, 2012, **7**, e38903.
52 A. Annunziata, M. E. Cucciolito, M. Di Ronza, G. Ferraro, M. Hadiji, A. Merlino, D. Ortiz, R. Scopelliti, F. Fadaei Tirani and P. J. Dyson, *Organometallics*, 2023, **42**(10), 952–964.
53 S. Singh, G. R. Navale, S. Agrawal, H. K. Singh, L. Singla, D. Sarkar, M. Sarma, A. R. Choudhury and K. Ghosh, *Int. J. Biol. Macromol.*, 2023, **239**, 124197.
54 S. L. Gras, L. J. Waddington and K. N. Goldie, *Protein Folding, Misfolding, and Disease: Methods and Protocols*, 2011, pp. 197–214.
55 S. La Manna, V. Roviello, P. L. Scognamiglio, C. Diaferia, C. Giannini, T. Sibillano, G. Morelli, E. Novellino and D. Marasco, *Int. J. Biol. Macromol.*, 2019, **122**, 517–525.
56 S. La Manna, P. L. Scognamiglio, V. Roviello, F. Borbone, D. Florio, C. Di Natale, A. Bigi, C. Cecchi, R. Cascella and C. Giannini, *FEBS J.*, 2019, **286**, 2311–2328.
57 C. Di Natale, D. Florio, S. Di Somma, A. Di Matteo, L. Federici, P. A. Netti, G. Morelli, A. M. Malfitano and D. Marasco, *Int. J. Biol. Macromol.*, 2020, **164**, 3501–3507.
58 S. La Manna, D. Florio, C. Di Natale, P. L. Scognamiglio, T. Sibillano, P. A. Netti, C. Giannini and D. Marasco, *Int. J. Biol. Macromol.*, 2021, **188**, 207–214.

59 K. L. Morris, A. Rodger, M. R. Hicks, M. Debulpaep, J. Schymkowitz, F. Rousseau and L. C. Serpell, *Biochem. J.*, 2013, **450**, 275–283.
60 S. Pushpakom, F. Iorio, P. A. Eyers, K. J. Escott, S. Hopper, A. Wells, A. Doig, T. Guilliams, J. Latimer and C. McNamee, *Nat. Rev. Drug Discovery*, 2019, **18**, 41–58.
61 K. M. Mahmud, M. S. Niloy, M. S. Shakil and M. A. Islam, *Pharmaceutics*, 2021, **13**, 1295.
62 S. Singh, G. R. Navale, S. Agrawal, H. K. Singh, L. Singla, D. Sarkar, M. Sarma, A. R. Choudhury and K. Ghosh, *Int. J. Biol. Macromol.*, 2023, 124197.
63 C. Di Natale, S. La Manna, A. M. Malfitano, S. Di Somma, D. Florio, P. L. Scognamiglio, E. Novellino, P. A. Netti and D. Marasco, *Biochim. Biophys. Acta, Proteins Proteomics*, 2019, **1867**, 637–644.
64 I. Haiduc, *J. Coord. Chem.*, 2020, **73**, 1619–1700.